Decoration of lipid vesicles by polyelectrolytes: mechanism and structure

Francois Quemeneur,[ab] Marguerite Rinaudo,[c] Georg Maret[b] and Brigitte Pépin-Donat*[a]

Received 24th March 2010, Accepted 27th May 2010
DOI: 10.1039/c0sm00154f

This study deals with 1,2-dioleoyl-sn-glycero-3-phosphocholine (DOPC) vesicles decorated with chitosan and hyaluronan, in dependence with respective membrane and polyelectrolyte net charges (tuned by pH). Studies are performed both on micrometric Giant Unilamellar Vesicles (GUVs) and on their nanometric Large Unilamellar Vesicle (LUV) homologues. Fluorescent microscopy observations reveal that GUVs are homogeneously decorated by both polyelectrolytes, even in the case where global charges of membrane and polyelectrolyte exhibit the same charge sign. ζ-Potential and light scattering experiments performed on LUVs suspensions upon chitosan addition are interpreted in terms of reversible aggregation of vesicles within the frame of a patch-like structure model. A similar aggregation–deaggregation mechanism is highlighted for GUVS in the presence of chitosan. Enthalpic variations measured by microcalorimetry and ζ-potential results show that the interaction between membrane and polyelectrolyte, previously demonstrated to be of electrostatic origin, is stronger when they are of opposite charge sign, as expected. For chitosan, the low saturation coverage degree is found to be nearly independent of molecular weight and interpreted in terms of polymer mainly adsorbed flat on the surface. On the contrary, maximum hyaluronan coverage degree dramatically varies with its molecular weight: hyaluronan is assumed to adsorb on the vesicle forming trains and loops. Finally, chitosan– and hyaluronan–vesicle decorations are demonstrated to be strongly resistant in a very large range of pH ($2.0 < pH < 10.0$).

1 Introduction

Vesicles, commonly referred as liposomes, have long been studied as models of biological membranes and especially at the micrometric scale of cells using Giant Unilamellar Vesicles (GUVs) of diameter ranging between 1 and 100 μm.[1] Smaller liposomes (Large Unilamellar Vesicles, LUVs; 100 < diameter < 500 nm) find various applications in pharmaceutical and cosmetic domains.[2] Thus, it is of interest to design smart liposomes either to better mimic living cells[3] or to adapt their physicochemical properties to specific applications.[4] Various macromolecules such as proteins and glycoconjugates interact with lipid bilayers to form the complex membrane of living cells.[5] Therefore, it is relevant to study the interaction of various polymers with vesicles to simulate cell–cell and cell–surface interactions.[6] Dealing with liposome applications, it is well known that polymer decoration may improve their structural stability,[7] biocompatibility and drug delivery efficiency.[8] Within this context, beside neutral poly(ethylene glycol) that in particular enhances liposome circulation time under *in vivo* conditions,[9] cationic polymers were used. As example, chitosan was recently employed to enhance liposomes' biocompatibility,[10] biodegradability[11] and mucoadhesivity.[12] As a possible alternative to these polymers, anionic polysaccharides such as heparin, which reduces the thrombogenicity of biomaterial surfaces,[13] or hyaluronan, which confers specific targeting character to coated liposomes for cancer therapy[14] and is biodegradable,[15] were suggested. Hyaluronan is also of interest to be a constituent of the extra-cellular matrix involved in the regulation of cell activity.[16]

In previous studies, it was shown that chitosan[17,18,19] and hyaluronan[15,20] interact with the zwitterionic phosphatidylcholine membrane of vesicles and that interactions are mainly of electrostatic origin. We have already demonstrated that the net charges of chitosan, hyaluronan and DOPC membrane depend on the pH and that varying this external parameter allows the screening of all the situations combining positively or negatively charged membrane and polyelectrolytes.[21] DOPC membrane is positively charged at pH = 2.0 due to quaternary amino groups, but progressively becomes negatively charged when pH becomes higher than 4.0,[19,22] due to the presence of phosphate groups, adsorbed negative counterions and/or carboxylic groups resulting from partial oxidation of lipids.[23] Hyaluronan is negatively charged at pH > 2.0, while chitosan is positively charged for pH < 6.5 and neutral for higher pH values.[24] We have already shown that, whatever the relative membrane and polyelectrolyte charge signs, chitosan and hyaluronan adsorb on liposomes, and that chitosan decoration enhances the stability of GUVs against salt and pH shocks.[18,19]

Dealing with the question of polyelectrolyte adsorption at the vesicle interface, a mechanism of interaction on surfaces of opposite charge was previously suggested in the literature.[25] It assumes the progressive formation of a more or less ordered patch-like (mosaic) surface structure consisting of a non-uniform distribution of the surface charges (domains of stuck charged polymer, *i.e.* with a local charge excess, alternating with domains of bare membrane surface). This leads to a progressive decrease of the global net charge of the vesicle upon adsorption of the

[a]*Laboratoire d'Electronique Moléculaire Organique et Hybride/UMR 5819 SPrAM (CEA-CNRS-UJF)/INAC/CEA-Grenoble, 38054 Grenoble Cedex 9, France. E-mail: brigitte.pepin-donat@cea.fr; Fax: +33 (0) 4 38 78 51 13; Tel: +33 (0) 4 38 78 38 06*
[b]*Physics Department, University of Konstanz, 78457 Konstanz, Germany*
[c]*Centre de Recherches sur les Macromolécules Végétales (CERMAV-CNRS) affiliated with Joseph Fourier University, BP53, 38041 Grenoble Cedex 9, France*

polyelectrolyte as observed recently on polylysine-decorated liposomes.[26] A short-range attractive potential[27,28] appears between negatively and positively charged domains of the patch-like surfaces of two separated vesicles leading to the formation of aggregates. In diluted liposome suspension, aggregates reach a maximum finite size at the isoelectric point resulting from a balance between long range electrostatic repulsion between liposomes with the same global charges and short range electrostatic attraction.[29] Additional adsorption of polyelectrolyte causes an overcharging effect with inversion of the net charge[30] of the polyelectrolyte-coated surface and the degree of aggregation decreases to isolated decorated vesicles. The overcharging effect goes to a limit due to the electrostatic barrier imposed by the excess of charges. It is clear that many factors play a role in this mechanism including the net charge of initial vesicles and polyelectrolyte, the structure of the adsorption sites, the salt concentration and solvent–polyelectrolyte interactions. In addition, it was suggested that at very low degrees of coverage, polyelectrolyte chains have a tendency to flatten, while at higher degree of coverage, they gradually may form loops and trains.[31]

This paper is devoted to a further understanding of the mechanisms of interaction between chitosan and hyaluronan polyelectrolytes and DOPC lipid vesicles, to the characterization of the structure of the decorated interface and to the direct observation of decoration stability under pH shocks. The use of LUVs and GUVs, of same lipid composition, allows us to perform experiments at various scales, which give complementary information. Firstly, we observe GUVs decoration by fluorescence microscopy. Secondly, the suspension state of LUVs and GUVs upon progressive decoration by chitosan is studied by ζ-potential, light scattering and microscopy experiments. Thirdly, we study the role of the polyelectrolyte molecular weight on its adsorption, and finally, the stability of polyelectrolyte decoration against pH shocks is investigated by confocal microscopy observation.

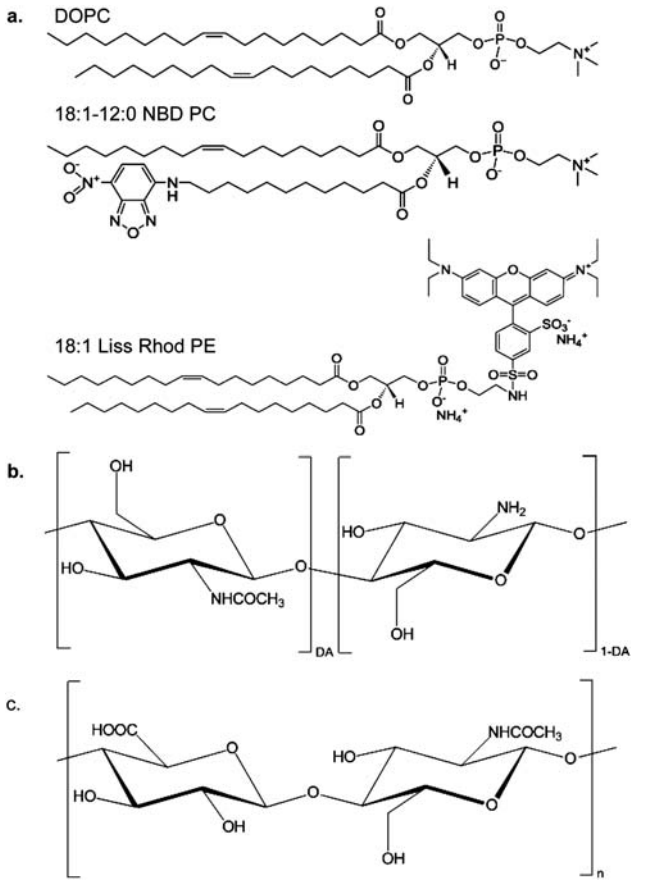

Fig. 1 Chemical structure of (a) used lipids and repeat units of the two polyelectrolytes studied: (b) Chitosan, positively charged polymer in acidic conditions (pH < 6.5) due to protonation of the $-NH_2$ groups; (c) Hyaluronan, anionic polymer at pH > 2.0 in relation with dissociation of carboxylic groups.

2 Experimental

2.1 Materials

The used zwitterionic lipids (Fig. 1a), 1,2-dioleoyl-sn-glycero-3-phosphocholine (DOPC) (M_w = 786.15), 1-oleoyl-2-[12-[(7-nitro-2-1,3-benzoxadiazol-4-yl)amino]dodecanoyl]-sn-glycero-3-phosphocholine (18 : 1–12 : 0 NBD PC) (M_w = 881.53) and 1,2-dioleoyl-sn-glycero-3-phosphoethanolamine-*N*-(lissamine rhodamine B sulfonyl) (ammonium salt) (18 : 1 Liss Rhod PE) (M_w = 1301.73) are purchased from Avanti Polar Lipids and dissolved separately as received in a chloroform–methanol solution (9/1 volume ratio) at 10 mg mL^{-1}. Fluorescent-labeled lipids are then mixed with DOPC in a weight ratio of 1/50 for the 18 : 1–12 : 0 NBD PC and 1/80 for the 18 : 1 Liss Rhod PE to a total concentration of 2 mg mL^{-1}. Solutions are kept at −20 °C until used. Sucrose, glucose, NaOH and HCl are purchased from Sigma-Aldrich. Highly purified 18.2 MΩ cm water is used for the preparation of all the solutions.

Chitosans (linear random copolymer of D-glucosamine and *N*-acetyl-D-glucosamine, Fig. 1b) with different weight-average molecular weights (M_w) and degrees of acetylation (DA) are used. Chitosan, $M_w = 5 \times 10^4$ and DA = 0.04, is provided by Primex; $M_w = 2.25 \times 10^5$ and DA = 0.05 is purchased from Sigma-Aldrich; $M_w = 5 \times 10^5$ and DA = 0.20 is purchased from Kitomer (Marinard, Canada). The maximum charge parameter[24] of these polyelectrolytes varies from $\lambda = 1.1$ (DA = 0.20) to 1.3 (DA = 0.04) when fully protonated (charge parameter corresponds to one charge per glucosamine moiety) with an intrinsic persistence length Lp around 10 nm.[32]

Hyaluronic acids (hyaluronan; linear alternated copolymer of D-glucuronic acid and *N*-acetyl-D-glucosamine, Fig. 1c) with different M_w (1.14×10^4, 4.1×10^4, 1.95×10^5, 6.63×10^5 and 1.8×10^6) are obtained by fermentation and purchased from ARD (Pomacle, France). The maximum charge parameter equals $\lambda = 0.72$ corresponding to one charge per disaccharide repeat unit with Lp around 8 nm.[16,33]

2.2 Preparation of giant and large unilamellar vesicles

GUVs are prepared from a mixture of DOPC and 18 : 1 Liss Rhod PE for the chitosan experiments or from a mixture of DOPC and 18 : 1–12 : 0 NBD PC for the hyaluronan experiments, using the standard electro-formation method:[34] a solution of lipids (2 mg mL^{-1}) is deposited on two glass plates of Indium Tin Oxide (ITO) and hydrated under an AC field with a 200 mM sucrose solution at ambient temperature.

LUVs are obtained by extrusion through a 0.2 μm filter of the GUVs previously produced by electroformation. LUVs prepared in these conditions are unilamellar[35] and their diameter is of the order of 200 ± 10 nm, encapsulating a 200 mM sucrose solution.

GUVs and LUVs are suspended in an external 200 mM sucrose solution containing HCl at controlled concentrations allowing the desired pH conditions (3.5 or 6.0). The exact lipid concentrations are determined in each vesicles sample by fluorescence in relation with the labeled lipid content.

2.3 ζ-Potential and dimension measurements

Measurements on vesicles suspensions corresponding to total lipid concentrations ranging between 3 and 5×10^{-3} mg mL^{-1} are performed at 20 °C with a commercial Zeta-sizer (Zetasizer NanoZS, Malvern, France). The measured electrophoretic mobility is transformed into ζ-potential values according to the Smoluchowski equation[36] and averaged over ten repeated measurements. This technique detects only vesicles in the range between 5 nm up to 10 μm (free polymer chains cannot be observed). The particle sizes are controlled *in situ* by light scattering measurements on extruded LUVs exhibiting a 200 ± 10 nm diameter and GUVS (selected with a diameter lower than 10 μm).

For each ζ-potential measurement, the following protocol is repeated: a given volume of solution (HCl, NaOH or polyelectrolyte) is added to the liposome suspension; after homogenization by stirring and 30 minutes incubation, we inject 1 mL of this mixture in the Zetasizer Nano Cell; the ζ-potential and average sizes of the dispersed liposomes are measured. After each measurement the whole solution is collected from the cell and reintroduced into the bulk solution (to keep a nearly constant volume of solution) before the addition of the next volume of polyelectrolyte solution. Those steps are repeated as many times as necessary.

2.4 Rate of decoration

We determine, by *in situ* fluorescence measurements performed at 20 °C with a Perkin Elmer luminescence spectrometer LS50B, the amount of lipids involved in the membranes of LUVs, assuming that no free lipids are present in solution. For polyelectrolytes (chitosan or hyaluronan), it is necessary to determine both the concentration of free polymer in solution and the amount adsorbed on the membrane (Γ). We assume as usual that, upon addition of very small amounts of polyelectrolyte into a vesicle suspension (with a membrane of opposite charge), the polyelectrolyte is fully adsorbed on the liposomes and relate the variation of ζ-potential to the amount of ionized groups (*i.e.* NH_3^+ and COO^- for chitosan and hyaluronan, respectively) fixed on the membrane. This allows calculation of the amount of polyelectrolyte adsorbed taking into account the protonation degree (controlled by pH) and acetylation degree (DA) in the case of chitosan.

The maximum amount of polyelectrolyte (Γ_{sat}) fixed on vesicles in large excess of free polyelectrolyte is defined as the maximum molar ratio of adsorbed chitosan monomeric units over lipid out. The degree of coverage is expressed in mass of polymer per unit surface of external membrane (with an area-per-lipid head of 0.725 nm^2).[37]

2.5 Isothermal titration microcalorimetry (ITC)

ITC measurements are realized at 20 °C using a Microcal VP-ITC titration microcalorimeter (Northampton, MA). LUVs suspension (0.2 mM lipid concentration) and chitosan (6.135 mM monomeric concentration) are prepared in 200 mM sucrose solution (described above) at both pH (3.5 and 6.0). Titration of chitosan adsorption is performed in a cell containing 1.447 mL of the LUV suspension, by 60 injections of 5 μL of the chitosan solution at a constant 300 rpm stirring rate. Each injection is performed over a period of 3 s. The heat flow is measured for up to 300 s before the subsequent injection takes place. The amount of heat produced per each chitosan injection is calculated by integration of the area under each individual peak by the instrument software, taking into account heat of dilution.

2.6 Polyelectrolyte fluorescent labeling and solution preparations

In order to observe the decoration of GUVs by polyelectrolytes, using fluorescence microscopy, we have labeled[38] chitosan ($Mw = 5 \times 10^5$) with fluorescein[19] and hyaluronan with rhodamine. For hyaluronan ($M_w = 6.63 \times 10^5$), 1 g is dissolved in 100 mL of 0.02 M NaCl and the pH is controlled at 6.1. After dissolution, 50 mL of methanol is added under stirring and directly after, 50 mg of tetramethylrhodamine B isothiocyanate (purchased from Sigma-Aldrich) dissolved in 50 mL of methanol is also added.

The degree of labeling is determined from the fluorescence intensity of diluted solutions of the free fluorescent probe compared with the fluorescence of a diluted solution of the labeled polysaccharides. It is found to be around 1 rhodamine per 25 disaccharide units (or 50 sugar units) for hyaluronan and 1 fluorescein per 60 sugar units for chitosan. These low percentages are chosen in order to minimize changes of the physical properties of the polyelectrolytes and lipid membrane assemblies by labeling.

Solutions of hyaluronan are prepared at 0.4 g L^{-1} by dissolving the polymer in 200 mM sucrose solution at pH = 6.0 while dissolution of cationic chitosan requires addition of stoichiometric amounts of HCl on the basis of $-NH_2$ content in the chitosan (final pH around 3.5). The solutions of polyelectrolyte are stirred for one night at room temperature until complete solubilization. The solutions of polyelectrolyte are diluted for vesicles' incubation and range between 0.1 to 0.01 g L^{-1} in a solution of 200 mM sucrose at pH = 3.5 or 6.0 and directly used.

2.7 GUVs incubated in polyelectrolyte solution for direct observation by optical microscopy

For GUVs incubation, the solutions of polyelectrolyte are used at 0.1 g L^{-1}, which is higher than the concentration of polyelectrolyte solution previously used for LUVs (0.01–0.05 mg mL^{-1}),[19] but we have checked by ζ-potential measurements that the initial concentration of polyelectrolyte solution, if between 0.01 and 0.1 g L^{-1}, does not modify the ζ-potential variation at a given molar ratio of polyelectrolyte repeat unit over accessible lipids. The GUV suspension is added to the polyelectrolyte solution and homogenized by successive aspirations with a pipette. This suspension is then left to rest during 30 min at room temperature for incubation.

2.8 Microscopy observations

Glass substrates are covered with a hydrophilic polymer, poly (ethylene glycol) (PEG), grafted covalently according to the protocol given by Zhang *et al.*,[39] in order to avoid their interaction with GUVs or polyelectrolytes. GUVs are transferred into the observation cell filled with a 200 mM glucose solution. The lower density of surrounding glucose solution causes sucrose-filled vesicles to sediment to the bottom of the cell.

We found that, whatever the polyelectrolyte, decorated GUVs always exhibit some loose interactions with the glass plate, probably due to a weak adhesion even after passivation of the surface with PEG.[39] It must be noted that in the absence of glass treatment, chitosan- and hyaluronan-decorated vesicles sediment, adhere and finally burst. pH shocks are imposed by injection of successive 5 μL additions of HCl or NaOH solutions at different initial concentrations in cell measurement (750 μL) in order to get at equilibrium the desired pH.

Phase contrast and fluorescence microscopy observations are made using an inverted microscope (Nikon, TE200, Tokyo, Japan) equipped with a 40X phase objective and a digital camera (NDIAG 1800; Diagnostic Instruments, Sterling Heights, MI). A mercury lamp provided the illumination for fluorescence experiments. A fluorescent block with filters EX 450–490 nm/BA 520 nm and a 505 nm dichroic mirror was used to observe the fluorescein-labelled chitosan decoration on DOPC GUVs.

Confocal microscopy observations are performed with an UltraView LCI Nipkow Disk scanner (PerkinElmer GmbH, Rodgau-Jügesheim, Germany) attached to a Zeiss Axiovert 200 microscope (Zeiss GmbH, Heidelberg, Germany) equipped with a C-Apochromat 63X, 1.2 NA water immersion objective. GUVs observations are made at 488 nm excitation using 500LP emission filters for the chitosan probed with fluorescein or 18 : 1–12 : 0 NBD PC lipids and at 568 nm excitation and 600/45BP emission filters for the hyaluronan labeled with rhodamine or 18 : 1 Liss Rhod PE lipids. Fluorescence acquisitions at these two excitation wavelengths are made successively.

3 Results and discussion

3.1. Decoration of GUVs by chitosan and hyaluronan: fluorescence confocal microscopy observation

GUVs are incubated with chitosan or hyaluronan at pH = 3.5 and 6.0 and observed by confocal imaging. Lipids and polyelectrolytes being labeled with different fluorescent probes, we can visualize successively and independently the lipid membrane and the polyelectrolyte decoration. Labeling of polyelectrolyte was already proved to not change ζ-potential variation of coated vesicles.[19] We now demonstrate in Fig. 2 that it is the same for labelling of lipids either by fluorescein (18 : 1–12 : 0 NBD PC) or rhodamine (18 : 1 Liss Rhod PE) whatever the pH. These results are in agreement with previously published data.[40] In addition, the inset of Fig. 2 shows that size of labelled or non-labelled bare vesicles remains constant in the accuracy limit between 2.5 < pH < 11.0. For extreme pH values (out of this range), size decrease is attributed to osmotic deflation.[41]

We recall that charge densities of both polyelectrolytes and DOPC membrane are strongly dependent on the pH. For the different cases of relative membrane/polyelectrolyte net charges

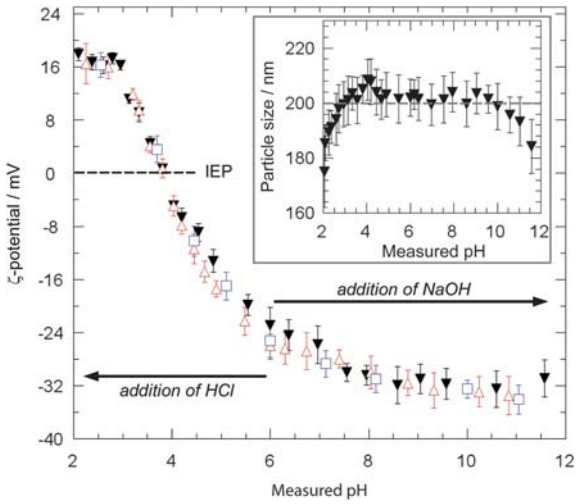

Fig. 2 ζ-potential variation of bare DOPC LUVs as a function of pH, without fluorescent labelling (solid black triangles) or including fluorescent probes: 18:1 Liss Rhod PE lipids in a weight ratio 1/80 (open red triangles) or 18:1-12:0 NBD PC lipids in a weight ratio 1/50 (open blue squares). Isolectric point (IEP) is obtained whatever the fluorescent labelling around pH = 4.0. Inset shows the particle size of DOPC LUVs upon pH variation.

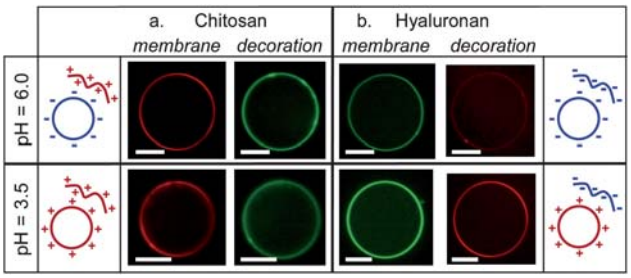

Fig. 3 Fluorescence confocal observations of a chitosan ($M_w = 5 \times 10^5$, DA = 0.20) and a hyaluronan ($M_w = 6.63 \times 10^5$) coated GUVs incubated either at pH = 3.5 or at pH = 6.0. For the same GUV, we visualize successively the lipid membrane and polyelectrolyte coating. The scale bars represent 10 μm. For each pH, sketches showing the membrane and the polyelectrolyte charge signs are indicated.

obtained at pH = 3.5 and 6.0, Fig. 3 shows independent observations of the fluorescent lipid bilayer and polymer decoration of GUVs coated by chitosan and hyaluronan: the whole surface of the vesicle looks homogeneously covered by polyelectrolytes without noticeable modification of GUV shape. Only a few heterogeneities are observed for chitosan decoration (and not for the membrane) at pH = 6.0 which may be attributed to adsorption of chitosan aggregates formed in solution because of its low solubility at this pH. A quantitative study of the azimuthal fluorescence profiles[42] of the non-decorated membrane (as reference) and of chitosan and hyaluronan decorated GUVs at pH = 3.5 or 6.0, averaged over twenty GUVs (data not shown), confirms lipid membrane and polyelectrolyte decoration homogeneity.

Direct comparison of coverage degrees is not possible from fluorescence intensities shown in Fig. 3 because optical recording parameters are not constant (laser intensity, camera exposure time) but adjusted to obtain optimal contrast. Moreover, the fluorescence efficiencies of fluorescein and rhodamine are pH-dependent.[43]

3.2. Role of polyelectrolyte sorption on suspension state of LUVs and GUVs

We stress again that the pH of both initial chitosan solutions and LUVs suspensions are strictly controlled and either equal to 3.5 or 6.0, to maintain the net charge of each component constant during all the experiments. Additionaly, the maximum of salt concentration is of the order of 10^{-4} M. Because interactions are mainly of electrostatic origin, added polyelectrolyte is expressed as the molar ratio of ionized groups ($-NH_3^+$ for chitosan and $-COO^-$ for hyaluronan) over lipids of the outer lipid layer (lipid out). At pH = 6.0, the membrane is negatively charged (ζ-potential ~ -20 mV), hyaluronan is strongly negatively charged (100% of the carboxylic groups are ionized)[44] and chitosan is partially positively charged (only 40% of the amino groups are protonated).[45] At pH = 3.5, the DOPC membrane is globally positively charged (ζ-potential $\sim +5$ mV), hyaluronan has a lower negative charge density (only 25% of the carboxylic groups are ionized) and chitosan is strongly positively charged (100% of the amino groups are protonated).

Firstly, the possible influence of the vesicle size on polyelectrolyte sorption is investigated by studying the variation of ζ-potential of LUVs (200 nm) and GUVs (~ 5 μm) as a function of added cationic chitosan ($M_w = 5 \times 10^5$, DA = 0.2) at pH = 6.0 (Fig. 4). For bare and slightly decorated GUVs, the negative ζ-potential is larger than that of LUVs. Nevertheless, this result is not ascribed to an influence of vesicle size on polyelectrolyte sorption but interpreted in terms of GUVs deformation due to the electric field.[46] Actually, because of their large size, GUVS are deformed to a prolate-like shape with a lower friction than the spherical corresponding vesicles, and then they present a larger mobility for the same surface charge state. An interesting point is that for a higher amount of added chitosan (roughly corresponding to the ζ-potential plateau), the ζ-potentials of LUVs and GUVs become similar which seems to indicate that, at maximum decoration, deformation of decorated GUVs decreases likely due to a membrane stiffness increase. This interpretation has been confirmed by AFM experiments.[47]

We now study the variation of ζ-potential and size of particles in suspension as a function of progressive addition of chitosan on DOPC membrane at pH = 3.5 and 6.0 (Fig. 5a). At pH = 6.0, we observe that upon first additions of the positively charged chitosan, the negative net charge of the vesicle is progressively decreased and tends towards zero. The isoelectric point (IEP, ζ-potential equals 0) occurs at $[NH_3^+]/[lipid\ out] \sim 0.18$ and corresponds to the neutralization of the global negative charge of the lipidic vesicles. From light scattering data, it is clearly shown that a maximum in size of particles present in solution for the partially chitosan-coated vesicles is obtained at the isoelectric point. We observe finite aggregates (absent in the case of bare vesicles—see Fig. 2 inset) with a maximum size around 800 nm (*i.e.* average diameter of aggregates/average diameter of vesicles around 4) without any observed flocculation over a few hours.

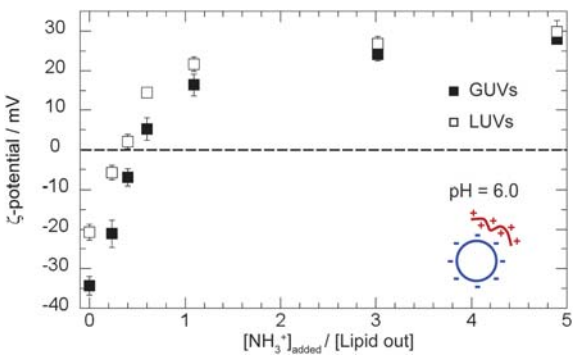

Fig. 4 ζ-potentials variation at pH = 6.0 of LUVs (open squares) and GUVs (solid squares) as a function of the added chitosan amount ($M_w = 5 \times 10^5$, DA = 0.20) expressed by the added molar ratio $[NH_3^+]$ / [lipid out] (ionized chitosan amino groups over accessible lipids of the membrane).

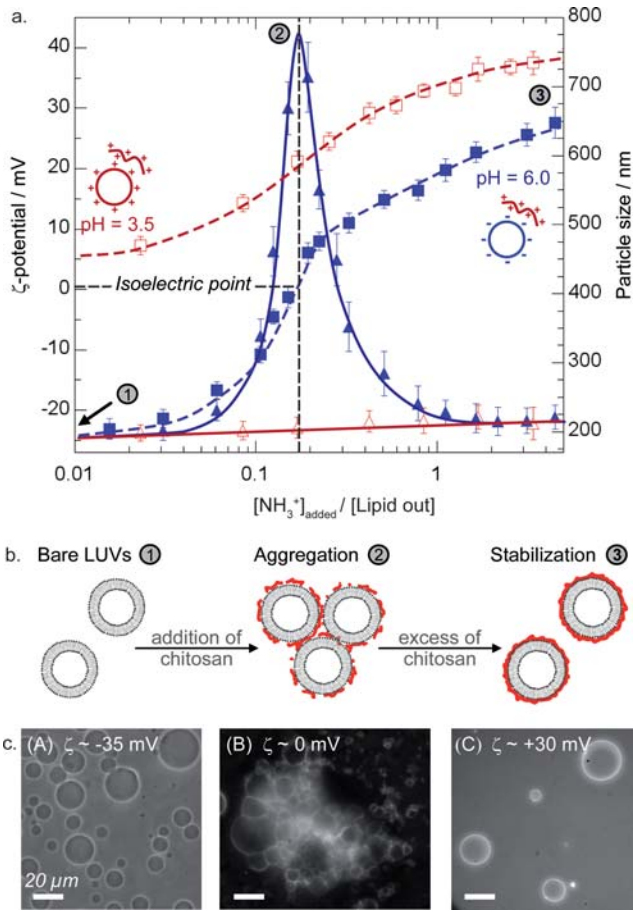

Fig. 5 (a) Variation of the ζ-potential (squares) and the particle diameter (triangles) of LUVs upon addition of chitosan, expressed by the molar ratio R = $[NH_3^+]$ / [lipid out] at pH = 6.0 and pH = 3.5. Open or solid signs are used when the initial charge signs of the membrane and polyelectrolytes are respectively the same or opposite, as detailed in the sketches for each pH. Lines are added to guide the eye and have no physical meaning. (b) Schematic LUVs suspension structure for three different cases of chitosan addition: (1) isolated bare LUVs when no chitosan is added, (2) LUVs aggregation when chitosan addition corresponds to the isoelectric point of the LUVs (ζ-potential = 0) and (3) isolated chitosan-coated LUVs when chitosan addition corresponds to coating saturation. (c) Similar aggregation-dissociation process is highlighted by microscopy observations on DOPC GUVs incubated, at pH = 6.0, with chitosan at different molar ratios R: (A) R = 0 (bare GUVs, ζ-potential ~ -35 mV), (B) R ~ 0.18 equivalent to the isoelectric point, and (C) R ~ 5 (ζ-potential ~ +30 mV) corresponding to the maximum of coating. The scale bars represent 20 μm.

Such an aggregation phenomenon was previously reported for similar systems (DPPG/polylysine[26] or DOTAP/polyacrylate[28]).

Upon addition of excess of chitosan, we observe that adsorption still occurs but aggregates are progressively dissociated with charge inversion to finally obtain isolated positively charged LUVs exhibiting the same dimensions as those of vesicles in the bare state. This result is attributed to an overcharging of the vesicles upon further chitosan addition, causing electrostatic repulsion. In our study, the concentration of chitosan at the adsorption plateau corresponds to the complete dissociation of aggregates allowing the study of isolated chitosan-coated vesicles. Schematic structures of the vesicle suspension for different chitosan additions are presented in Fig. 5b: state (1) corresponds to initial isolated bare vesicles, state (2) to aggregated decorated vesicles at the isoelectric point and state (3) to isolated highly decorated vesicles. This particle association–dissociation mechanism results from the equilibrium between long range repulsion and short range attraction, all of electrostatic nature, in good agreement with a patch-like structure assumed for the decorated membrane.[28]

The same results were interestingly obtained on micrometric vesicles upon addition of chitosan: Fig. 5c shows the direct observation of bare GUVs (A), GUVs aggregation at isoelectric point (B) and isolated highly decorated GUVs (C) (corresponding to the ζ-potential plateau), which result from aggregate dissociation. The interesting conclusion is that, in excess of chitosan, decorated vesicles are isolated allowing the testing of their intrinsic physico-chemical properties.[47,48]

On the contrary and as expected when the experiment is performed at pH = 3.5, where both bare vesicles and chitosan are positively charged, adsorption is demonstrated by ζ-potential variation but without any vesicle charge inversion nor vesicle aggregation upon addition of chitosan due to the increase of the net charge leading to stabilization of the suspension (see Fig. 5a).

Considering this series of results, we can claim that: i) the size of the vesicles (in a range from nm to μm) does not play any role on the maximum polyelectrolyte decoration and ii) upon progressive addition of chitosan, the same behavior is observed for LUVs and GUVs suspensions at pH = 6.0 with, successively, aggregation around the isoelectric point and further redispersion in excess chitosan.

3.3 Influence of polyelectrolyte molecular weight and relative membrane-polymer net charges on adsorption

The coverage degree of substrates by polymers may vary or not as a function of polymer structure and molecular weight, depending on whether polymers adsorb flat or forming trains and loops at the external membrane surface. In our previous studies,[21] ζ-potential variation of DOPC vesicles upon chitosan and hyaluronan addition was interpreted in terms of the amount of polyelectrolyte charges adsorbed and, consequently, to their degree of coverage. Therefore, in order to get information on the conformation of polyelectrolyte adsorbed on vesicles, we study successively ζ-potential variation of liposomes as a function of chitosan and hyaluronan molecular weights.

In the following, the difference between the measured ζ-potential and the value of the ζ-potential of the bare lipid membrane (Δζ) is considered in order to only observe the decoration contribution to ζ-potential variation.

a. Chitosan adsorption. We first examine the role of chitosan molecular weight on its adsorption. Three chitosans with different molecular weights and degrees of acetylation are used: $M_w = 5 \times 10^4$ (DA = 0.04), 2.25×10^5 (DA = 0.05), and 5×10^5 (DA = 0.20). Fig. 6 presents, at pH = 6.0 and 3.5, respectively, the variation of the Δζ of liposomes observed in the presence of the three chitosans as function of the added polymer amount expressed by the molar ratio $[NH_3^+]/[lipid\ out]$, which accounts for acetylation degree.

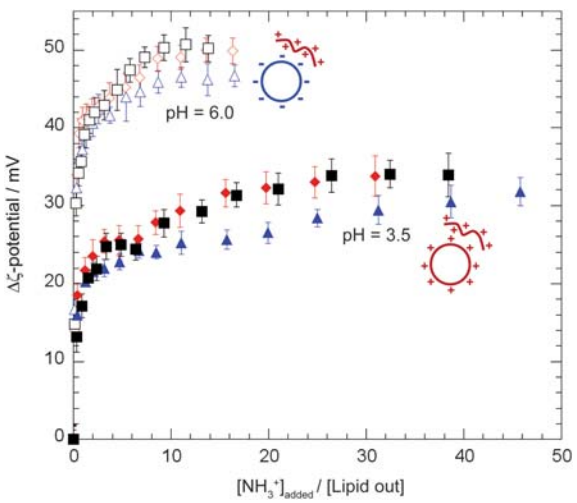

Fig. 6 Influence of the chitosan molecular weight (M_w) on the variation of the ζ-potentials of LUVs at pH = 6.0 (open symbols) and pH = 3.5 (solid symbols). The evolution of the Δζ is shown as a function of the molar ratio [NH_3^+] / [lipid out] (ionized chitosan amino groups over accessible lipids of the membrane) for 3 different M_w: 5×10^4 (triangles), 2.25×10^5 (diamonds), and 5×10^5 (squares).

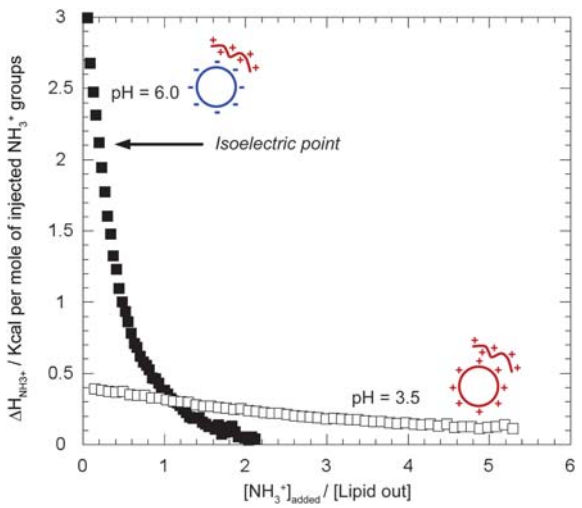

Fig. 7 Influence of the membrane and chitosan net charges on the enthalpic variation upon polyelectrolyte adsorption. The evolution of the molar enthalpy for each successive chitosan addition is shown as a function of the molar ratio [NH_3^+] / [lipid out] for $M_w = 2.25 \times 10^5$, DA = 0.05 at pH = 3.5 (open symbols) and pH = 6.0 (solid symbols).

For all chitosan molecular weights, ζ-potential variation displays the same general trend as previously observed:[21] a sharp increase at low concentration of added chitosan, followed by a smooth variation before reaching a constant value for a large excess of polymer. Fig. 6 shows that, for both pH values (3.5 and 6.0), the maximum value of ζ-potential (*i.e.* $\Delta\zeta_{max}$) observed at the plateau only slightly varies with M_w: *i.e.* the total amount of ionized chitosan amino groups fixed on the lipid membrane, at a given pH, is nearly independent of the molecular weight. At pH = 6.0 (negative membrane/positive polyelectrolyte), curves of ζ-potential variation as a function of added chitosan are superimposed for the three chitosan molecular weights; plateau values ($\Delta\zeta_{max} \sim +49$ mV) are obtained for the same ratio $[NH_3^+]/[lipid\ out] > 5$. These results are in good agreement with a flat adsorption of chitosans with a thickness of the adsorbed layer which does not displace significantly the shear plane.

At pH = 3.5 (positively charged membrane and polyelectrolyte), a larger amount of chitosan (highly soluble because fully protonated), which depends on M_w, is necessary to get the plateau ($\Delta\zeta_{max} \sim +33$ mV): $[NH_3^+]/[lipid\ out] \sim 15$ for the higher molecular weights ($M_w = 2.25 \times 10^5$ and 5×10^5), but $[NH_3^+]/[lipid\ out] \sim 45$ for $M_w = 5 \times 10^4$. These results may be interpreted in terms of looser interactions when polyelectrolyte and membrane have the same charge sign. In the case of the low molecular weight chitosan we suggest that it adsorbs flat on the surface due to its high charge density and its stiffness (contour length around 10 times Lp) while interacting with the negative charges on the membranes. Dealing with higher molecular weight chitosans, they stick on the surface as charged wormlike chains and form loops with locally higher charge density at the interface; then saturation occurs more rapidly.

Calorimetric titration experiments are performed at pH = 3.5 and 6.0 in order to further study the interaction between DOPC lipid membrane and chitosan ($M_w = 2.25 \times 10^5$). Fig. 7 presents the variation of enthalpy $\Delta H_{NH_3^+}$ expressed in kcal per mole of injected NH_3^+, as a function of $[NH_3^+]/[lipid\ out]$ at both pH values. At pH = 6.0, when oppositely charged chitosan and membrane interact, a large enthalpic effect occurs for the first amounts of chitosan added for which no aggregation occurs ($[NH_3^+]/[lipid\ out] < 0.1$, see Fig. 5a). Upon further additions, enthalpic variations decrease progressively and tend to very small values for $[NH_3^+]/[lipid\ out] > 2.2$ (this value is much larger than 0.18 obtained at the isoelectric point) which correspond to the ζ-potential plateau when decorated membrane and polyelectrolyte are both positively charge. The $\Delta H_{NH_3^+}$ measured also includes association–dissociation of vesicles (see Fig. 5a) in the intermediate regime of chitosan addition. This behavior reflects the overcharging effect with formation of the electrostatic barrier limiting further adsorption.

At pH = 3.5, the enthalpic effect still exists, indicating that interaction still occurs although both membrane and chitosan are initially positively charged. Nevertheless, it is dramatically lower than at pH = 6.0 and decreases very smoothly, indicating that the limit of fixation should be obtained for a much larger excess of chitosan as observed for ζ-potential measurements (Fig. 6). This indicates that *positive chitosan amino groups* interact with negative groups present on the membrane even if a long range electrostatic repulsion exists between the globally positive membrane and positive chitosan. In addition, attractive forces may involve hydrophobic and hydrogen-bond interactions.[49]

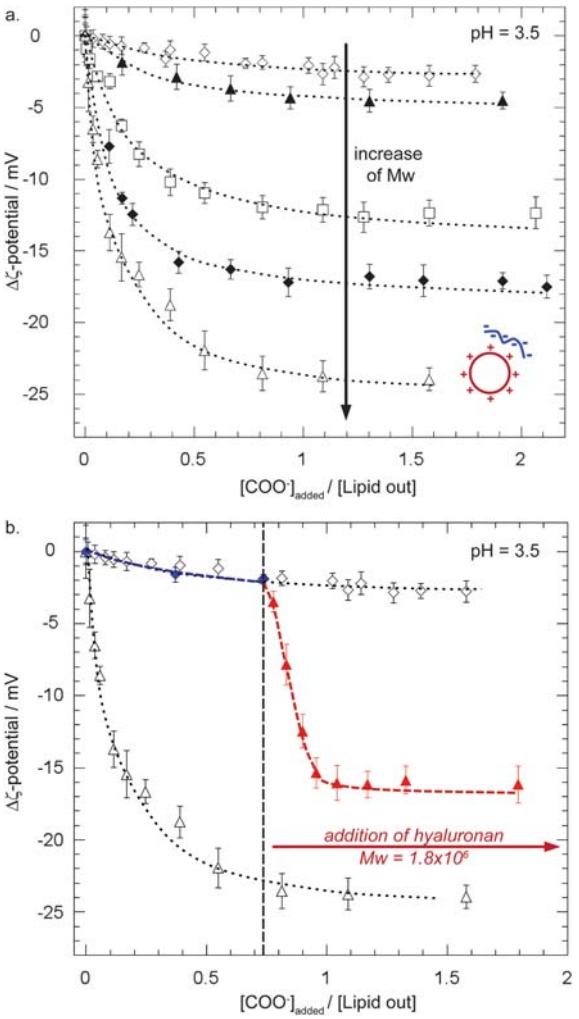

Fig. 8 (a) Influence of the hyaluronan molecular weight (M_w) on the variation of the ζ-potentials of LUVs at pH = 3.5. The evolution of the Δζ is shown as a function of the molar ratio [COO^-] / [lipid out] for 5 different M_w: 1.14×10^4 (open diamonds), 4.1×10^4 (solid triangles), 1.95×10^5 (open squares), 6.63×10^5 (solid diamonds) and 1.8×10^6 (open triangle). (b) Influence of a partial coating by a low molecular weight ($M_w = 1.14 \times 10^4$, solid blue diamonds) on the adsorption of a high molecular weight ($M_w = 1.8 \times 10^6$, solid red triangles) on liposomes. The evolution of the Δζ is compared with previous results obtained for $M_w = 1.14 \times 10^4$ (open diamonds) and 1.8×10^6 (open triangles) in (a). The dotted lines are added to guide the eye and have no physical meaning.

Table 1 Influence of molecular weight and pH on maximum amount of adsorbed chitosan on DOPC vesicles expressed as Γ_{sat} (maximum molar ratio of chitosan monomeric units over lipid out) and related coverage degrees (see section 2.4)

pH	M_w/g mol^{-1}	$\Gamma_{sat} \pm 0.01$	Coverage degree/mg m^{-2}
3.5	5×10^4	0.20	0.07
	2.25×10^5	0.22	0.08
	5×10^5	0.22	0.08
6.0	5×10^4	0.30	0.11
	2.25×10^5	0.32	0.12
	5×10^5	0.32	0.12

Table 2 Influence of molecular weight at pH = 3.5 on maximum amount of adsorbed hyaluronan on DOPC vesicles expressed as Γ_{sat} (maximum molar ratio of hyaluronan repeat units and lipid out) and related coverage degrees (see section 2.4). Values given at pH = 6.0 are obtained from previous published data.[21]

pH	M_w/g mol^{-1}	$\Gamma_{sat} \pm 0.04$	Coverage degree/mg m^{-2}
3.5	1.14×10^4	0.12	0.11
	4.1×10^4	0.21	0.19
	1.95×10^5	0.51	0.47
	6.63×10^5	0.71	0.65
	1.8×10^6	0.97	0.90
6.0	6.63×10^5	0.41	0.36

From ζ-potential values, we get the maximum amount of adsorbed chitosan expressed as Γ_{sat} (maximum molar ratio of adsorbed chitosan monomeric units and lipid out) and the coverage degree (see section 2.4). Table 1 gives Γ_{sat} and coverage degrees determined for the different molecular weights at pH = 3.5 and 6.0.

As expected, larger adsorption occurs at pH = 6.0 than at pH = 3.5 whatever the molecular weight. Taking into account that fluorescent microscopy observations reveal a homogeneous coverage, the chitosan-decorated surface of the vesicle may be regarded as a homogeneous patch-like layer formed of domains of chitosan chains adsorbed flat on the interface. The surface covered by these domains represents 10% of a virtual monolayer formed by a compact arrangement of chains, assuming that a chitosan monomeric unit occupies an area of 0.25 nm^2.

b. Hyaluronan adsorption. The adsorption of hyaluronan is only studied at pH = 3.5, corresponding to a membrane with a low positive charge (+ 5 mV) and negatively charged polyelectrolyte. The role of hyaluronan molecular weight is observed: five hyaluronans exhibiting different molecular weights are used: $M_w = 1.14 \times 10^4$, 4.1×10^4, 1.95×10^5, 6.63×10^5 and 1.8×10^6. Fig. 8 shows the variation of the Δζ for these five different samples as a function of the added amount of hyaluronan. Contrary to chitosan results, the total variation of ζ-potential ($\Delta\zeta_{max}$) is strongly dependant on the molecular weight: the higher the molecular weight, larger is the $\Delta\zeta_{max}$. It must be recalled that the charge density of hyaluronan at pH = 3.5 is low (only 0.25 charge per disaccharide repeat unit) and its flexibility is larger than that of chitosan. These two parameters may cause a difference in adsorption if compared to chitosan. From ζ-potential values, we determine the maximum amount of adsorbed hyaluronan expressed as Γ_{sat} (maximum molar ratio of adsorbed hyaluronan repeat units over lipid out) and the coverage degree (see section 2.4). Table 2 gives Γ_{sat} and coverage degrees determined for the different molecular weights at pH 3.5.

The degree of coverage for hyaluronan is much larger than for chitosan and strongly varies with molecular weight at pH = 3.5.

Taking into account that fluorescent microscopy observations reveal a homogeneous coverage (Fig. 3), and that the adsorption depends on M_w, the external surface of hyaluronan-decorated vesicles may be regarded as a homogeneous distribution of decorated domains composed of trains and loops with an average low density in polyelectrolyte monomeric units. Exceptions may occur for the lowest molecular weight which behaves as a stiff molecule with a contour length equal to 3 Lp. Actually, assuming a monolayer formed by side-by-side repeat unit compact coverage (0.5 nm^2 each dissaccharide), the maximum degree of hyaluronan coverage should be equal to 1.34 mg m^{-2}. Of course, such a model of repeat units stacking to form a dense monolayer is unrealistic; the degree of coverage given in Table 2 for the highest molecular weight (much larger in this case than for chitosan) is of the same order of magnitude as that expected from this unrealistic model. This further confirms the presence of hyaluronan loops and trains at the surface of the vesicle. We are aware that loop formation may displace the shear plane and lead to underestimation of ζ-potential values and then, of Γ_{sat} and the coverage degree.[50]

Similar vesicle aggregation–deaggregation processes, as described for chitosan at pH = 6.0 (Fig. 5), are observed with hyaluronan at pH = 3.5 (in both cases, membrane and polyelectrolyte have opposite charge sign). For hyaluronan, the maximum aggregate size obtained at the isoelectric point (for a ratio $[COO^-]/[lipid\ out] = 0.11$) is around 900 nm for $M_w = 6.63 \times 10^5$ (*i.e.* average diameter of aggregates/average diameter of vesicles is around 4).

In Table 2, we observe that the degree of coverage at pH = 6.0, where membrane and hyaluronan are both negatively charged, is lower than at pH = 3.5 as expected.

In order to further confirm the crucial role of the molecular weight, we have performed the following experiment: we partially decorate the membrane with the low molecular weight hyaluronan ($M_w = 1.14 \times 10^4$) up to $\Gamma = 0.07$ (see Fig. 8b) and we observe exactly the same ζ-potential variation as observed in the previous experiment (Fig. 8a) which points out the good reproducibility of the measurements. Then, when we reach a ratio $[COO^-]/[lipid\ out] = 0.7$ added, we stop adding hyaluronan of $M_w = 1.14 \times 10^4$ and add progressive amounts of hyaluronan with higher molecular weight ($M_w = 1.8 \times 10^6$). We observe a sharp decrease of the ζ-potential indicating an additional adsorption of the hyaluronan of higher molecular weight. Nevertheless, in an excess of high hyaluronan molecular weight, ζ-potential does not reach the expected value of −25 mV ($\Gamma_{sat} = 0.97$) obtained previously for $M_w = 1.8 \times 10^6$ alone. We interpret this result assuming that the hyaluronan fraction of low molecular weight remain adsorbed and is not displaced by the higher molecular weight hyaluronan in the time scale of our experiments (few hours). The remaining available surface limits the adsorption of the high molecular weight hyaluronan.

3.5. Stability of hyaluronan and chitosan decoration against pH shocks

Chitosan-decorated vesicles have been demonstrated to be more stable than bare vesicles in extreme pH conditions.[18,19] The same results are obtained for hyaluronan-decorated vesicles (data not shown). From these behaviors, it was assumed that decoration remains in extreme pH conditions. We now want to directly confirm this assumption, *i.e.* to observe that even when hyaluronan and chitosan ionization are repressed at extreme acid and basic pH conditions, respectively, decoration remains. For that purpose, we observe hyaluronan and chitosan-decorated GUVs by confocal microscopy over a large range of pH (from 2.0 to 10.0). The vesicle decoration is performed in conditions where membrane and polyelectrolyte are oppositely charged (strongest affinity).

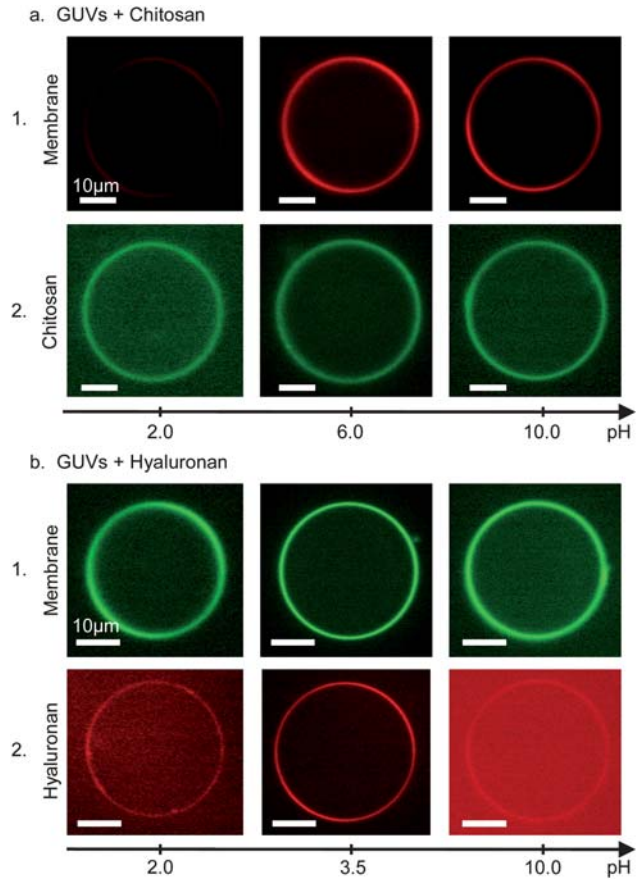

Fig. 9 Confocal microscopy observation of GUVs of the same sizes, coated with chitosan ($M_w = 5 \times 10^5$, DA = 0.20) at pH = 6.0 (a) or with hyaluronan ($M_w = 6.63 \times 10^5$) at pH = 3.5 (b) (column 2) and then subjected to pH shocks, either down to pH = 2.0 or up to pH = 10.0. We simultaneously visualize for each GUVs the lipid membrane (line 1) and the polyelectrolyte coating (line 2) for the three pH values. The scale bars represent 10 µm.

Chitosan-decorated vesicles are incubated at pH = 6.0 for a ratio $[NH_3^+]/[lipid\ out] \sim 9$ corresponding to a coverage degree of 0.12 mg m^{-2}; in the case of hyaluronan, vesicles are incubated at pH = 3.5 with a ratio $[COO^-]/[lipid] \sim 12$ and a coverage degree of 0.65 mg m^{-2}. These values correspond to the adsorption saturation. For the different values of pH, we visualize independently the lipid membrane and the polyelectrolyte decoration (respectively lines 1 and 2 of Fig. 9 for chitosan and hyaluronan). We observe that, in this wide range of pH (from 2.0 to 10.0), the membrane remains undamaged, and chitosan or hyaluronan remains adsorbed. Nevertheless, no quantitative comparison of coverage degrees from fluorescence intensity analysis can be performed from this figure as previously explained. For extreme pH values, where attractive electrostatic contributions are reduced, hydrogen bonds and hydrophobic attractions have a greater contribution to polyelectrolyte–membrane association.

3.6 Characterization of polyelectrolyte decoration: comparison between chitosan and hyaluronan

a. Degree of coverage. To compare more easily hyaluronan and chitosan results, Fig. 10 presents the degree of coverage

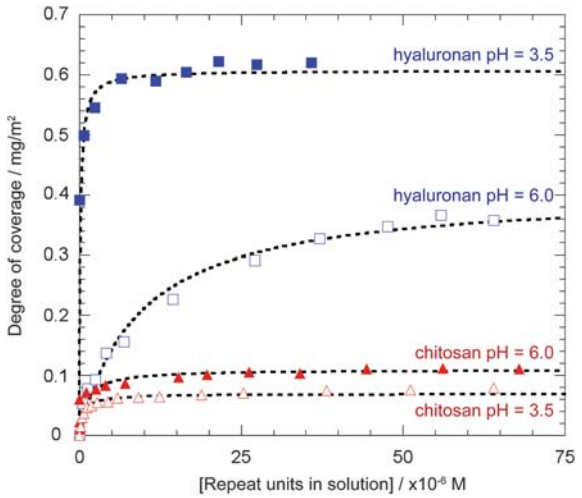

Fig. 10 Degree of coverage for chitosan ($M_w = 5{\times}10^5$, DA = 0.20; triangles) and hyaluronan ($M_w = 6.63 \times 10^5$; squares) as function of the repeat unit concentration of polyelectrolyte free in solution at pH = 3.5 and 6.0. Open or solid signs are used when the charge signs of the membrane and polyelectrolytes are the same or opposite respect.

deduced from ζ-potential measurements as a function of free polyelectrolyte in the suspension for similar M_w (*i.e.* chitosan $M_w = 5 \times 10^5$ and hyaluronan $M_w = 6.63 \times 10^5$) at pH = 3.5 and 6.0. For both polyelectrolytes, the degree of coverage is higher when the charge sign of the polyelectrolyte and membrane are opposite than when they exhibit the same charge sign. A smaller amount of polyelectrolyte is needed to get the plateau in the case of oppositely charged membrane and polyelectrolyte. An other sticking point is that for chitosan the degree of coverage is always much lower than for hyaluronan.

b. Conformation of polyelectrolytes at interface. For both polyelectrolytes, fluorescence microscopy shows that a homogeneous layer adsorbs at the micrometric scale. Based on experimental data reported in this paper, we assume that, at the nanometric scale, the decoration is made of charged domains where polyelectrolyte adsorbed flat (chitosan) or forms loops and trains (hyaluronan) on the basis of the molecular weight dependence.

With chitosan, whatever the molecular weight, in excess of polymer, the decorated vesicle is always highly positively charged. With hyaluronan, on the other hand, in excess of polyelectrolyte, the negative global charge of the coated vesicles is dependant on its molecular weight.

Conclusions

In this paper we have pointed out the difference between hyaluronan and chitosan interaction with lipid membranes. Fluorescent observations confirm that polyelectrolytes interact with zwitterionic DOPC membrane giving rise to homogeneous decoration, at the micrometric scale, even when polyelectrolyte and membrane exhibit the same charge sign.

In the case of membrane and polyelectrolyte of opposite charge, chitosan is demonstrated to adsorb flat on the vesicle surface with a maximum coverage degree of the order of

0.12 mg m^{-2}, while hyaluronan with $M_w > 10^4$ forms loops and trains with a maximum coverage degree depending on M_w and ranging between 0.19 up to 0.90 mg m^{-2}. Hyaluronan of very low M_w is assumed to adsorb flat on the membrane with a degree of coverage of 0.11 mg m^{-2}. At pH = 3.5, when the membrane and chitosan have the same charge sign, the degree of coverage and energy of interaction are lower (it is the same case for hyaluronan at pH = 6.0), and it is suggested that polymers with M_w higher than 5×10^4 form few loops.

In addition, the presence of chitosan or hyaluronan decoration on the zwitterionic membrane in a wide range of pH (from 2.0 to 10.0) is demonstrated and is responsible for the stability of decorated vesicles previously reported under pH shocks.

The formation of aggregates of both LUVs and GUVs upon a low degree of decoration by a polyelectrolyte of opposite charge, followed by the aggregates' dissociation and stabilization of isolated decorated vesicles in excess polyelectrolyte is interpreted within the frame of a patch-like submicronic structure made of non-uniform charged domains on the surface created by the adsorption of polyelectrolyte.

We have demonstrated that the control of the chemical structure, charge density, stiffness and molecular weight of hyaluronan and chitosan used to decorate the vesicles allow us to tune their net charge which governs the interactions with various biological systems and other substrates.

Such pH-resistant vesicles decorated by biocompatible and biodegradable polyelectrolytes hold promise for new potential applications.

Acknowledgements

We acknowledge financial support by the International Research Training Group 667 "Soft Matter Physics of Model Systems" and the German-French University (UFA-DFH) Saarbrücken. We thank our colleagues Omar Mertins, Carlos Marques, André Schroder and Jeorg Baschnagel at Institut Charles Sadron, Université de Strasbourg, France, for constructive discussion.

Notes and references

1 R. Lipowsky and E. Sackmann, *Structure and dynamics of Membranes, Handbook of Biological Physics Vol. 1A and 1B*, Elsevier science B.V., Amsterdam, 1995.
2 K. A. Edwards and A. J. Baeumner, *Talanta*, 2006, **68**, 1432–1441.
3 V. Noireaux and A. Libchaber, *Proc. Natl. Acad. Sci. U. S. A.*, 2004, **101**, 17669–17674; A. P. Liu and D. A. Fletcher, *Nat. Rev. Mol. Cell Biol.*, 2009, **10**, 644–650.
4 D. Felnerova, J.-F. Viret, R. Gluck and C. Moser, *Curr. Opin. Biotechnol.*, 2004, **15**, 518–529; T. M. S. Chang, *Artif. Cells, Blood Substitutes, Biotechnol.*, 2006, **34**, 551–566.
5 S. Sabri, M. Soler, C. Foa, A. Pierres, A.-M. Benoliel and P. Bongrand, *J. Cell Sci.*, 2000, **113**, 1589–1600.
6 P. F. Yang, D. Major and U. Rutishauser, *J. Biol. Chem.*, 1994, **269**, 23039–23044.
7 M. Maeda, A. Kumano and D. A. Tirrell, *J. Am. Chem. Soc.*, 1988, **110**, 7455–7459; A. A. Yaroslavov, O. Y. Kuchenkova, I. B. Okuneva, N. S. Melik-Nubarov, N. O. Kozlova, V. I. Lobyshev, F. M. Menger and V. A. Kabanov, *Biochim. Biophys. Acta, Biomembr.*, 2003, **1611**, 44–54; P. M. Macdonald, K. J. Crowell, C. M. Franzin, P. Mitrakos and D. Semchyschyn, *Solid State Nucl. Magn. Reson.*, 2000, **16**, 21–36; C. Ladavière, C. Tribet and S. Cribier, *Langmuir*, 2002, **18**, 7320–7327; L. Y. Wang, M. Schonhoff and H. Mohwald, *J. Phys. Chem. B*, 2002, **106**, 9135–9142; L. Ramos, M. Schonhoff, Y. Luan and H. Mohwald, *Colloids Surf., A*, 2007, **303**, 79–88; C. Hiergeist and R. Lipowsky, *J. Phys. II*, 1996, **6**, 1465–1481; E. Helfer, S. Harlepp, L. Bourdieu, J. Robert, F. C. MacKintosh and D. Chatenay, *Phys. Rev. E: Stat., Nonlinear, Soft Matter Phys.*, 2001, **63**(2), 021904; V. Nikolov, R. Lipowsky and R. Dimova, *Biophys. J.*, 2007, **92**, 4356–4368.
8 T. Xu, N. Zhang, H. L. Nichols, D. Shi and X. Wen, *Mater. Sci. Eng., C*, 2007, **27**, 579–594.
9 D. C. Drummond, O. Meyer, K. Hong, D. B. Kirpon and D. Papahadjopoulos, *Pharm. ReV.*, 1999, **51**, 691–743.
10 L. B. Maron, C. P. Covas, N. P. Da Silveira, A. Pohlmann, O. Mertins, L. N. Tatsuo, O. A. B. Sant'anna, A. M. Moro, C. S. Takata, P. S. de Araujo and M. H. B. da Costa, *J. Liposome Res.*, 2007, **17**, 155–163.
11 D. L. Elbert and J. A. Hubbell, *Annu. Rev. Mater. Sci.*, 1996, **26**, 365–394.
12 H. Takeuchi, H. Yamamoto, T. Niwa, T. Hino and Y. Kawashima, *Pharm. Res.*, 1996, **13**, 896–901; P. Perugini, I. Genta, F. Pavanetto, B. Conti, S. Scalia and A. Baruffini, *Int. J. Pharm.*, 2000, **196**, 51–61; J. Thongborisute, H. Takeuchi, H. Yamamoto and Y. Kawashima, *J. Lipid Res.*, 2006, **16**, 127–141; W. X. Ding, X. R. Qi, Q. Fu and H. S. Piao, *Drug Delivery*, 2007, **14**, 101–104; J. Zhang and S. Wang, *Int. J. Pharm.*, 2009, **372**, 66–75.
13 A. G. Kidane, H. Salacinski, A. Tiwari, K. R. Bruckdorfer and A. M. Seifalian, *Biomacromolecules*, 2004, **5**, 798–813; J. F. Kocsis, G. Llanos, E. Holmer and J. Long-Term, *Eff. Med. Implants*, 2000, **10**, 19–45.
14 D. Peer and R. Margalit, *Neoplasia*, 2004, **6**, 343–353; C. Surace, S. Arpicco, A. Dufay-Wojcicki, V. Marsaud, C. Bouclier, D. Clay, L. Cattel, J.-M. Renoir and E. Fattal, *Mol. Pharmaceutics*, 2009, **6**, 1062–1073; T. Kaasgaard and T. L. Andresen, *Expert Opin. Drug Delivery*, 2010, **7**, 225–243.
15 A. Taglienti, F. Cellesi, V. Crescenzi, P. Sequi, M. Valentini and N. Tirelli, *Macromol. Biosci.*, 2006, **6**, 611–622.
16 *Hyaluronan, vol. 1: Chemical, biochemical and biological aspects; Hyaluronan, vol 2: Biomedical, medical and clinical aspects*, ed. J. F. Kennedy, G. O. Phillips, P. A. Williams and V. C. Hascall, Woodhead Pub., Abington (UK), 2002.
17 Henriksen, S. R. Vagen, S. A. Sande, G. Smistad and J. Karlsen, *Int. J. Pharm.*, 1997, **146**, 193–204; I. Henriksen, G. Smistad and J. Karlsen, *Int. J. Pharm.*, 1994, **101**, 227–236; F. J. Pavinatto, A. Pavinatto, L. Caseli, D. S. dos SantosJr., T. M. Nobre, M. E. D. Zaniquelli and O. N. de OliveiraJr, *Biomacromolecules*, 2007, **8**, 1633–1640; F. J. Pavinatto, L. Caseli, A. Pavinatto, D. S. dos SantosJr., T. M. Nobre, M. E. D. Zaniquelli, H. S. Silva, P. B. Miranda and O. N. de Oliveira Jr., *Langmuir*, 2007, **23**, 7666–7671; O. Mertins, P. H. Schneider, A. R. Pohlmann and N. Pesce da Silveira, *Colloids Surf., B*, 2010, **75**, 294–299.
18 F. Quemeneur, A. Rammal, M. Rinaudo and B. Pépin-Donat, *Biomacromolecules*, 2007, **8**, 2512–2519.
19 F. Quemeneur, M. Rinaudo and B. Pépin-Donat, *Biomacromolecules*, 2008, **9**, 396–402.
20 F. Quemeneur, M. Rinaudo and B. Pépin-Donat, *Biomacromolecules*, 2008, **9**, 2237–2243.
21 M. Rinaudo, F. Quemeneur and B. Pépin-Donat, *Macromol. Symp.*, 2009, **278**, 67–79.
22 A. D. Petelska and Z. A. Figaszewski, *Biophys. J.*, 2000, **78**, 812–817.
23 P. L. Luisi and P. Walde, *Giant Vesicle*; John Wiley & Sons: New York, 2002; pp 108–112.
24 M. Rinaudo, *Prog. Polym. Sci.*, 2006, **31**, 603–632.
25 J. Gregory, *J. Colloid Interface Sci.*, 1973, **42**, 448–456; J. X. Mou, D. M. Czajkowsky, Y. Y. Zhang and Z. F. Shao, *FEBS Lett.*, 1995, **371**, 279–282; A. V. Dobrynin, A. Deshkovski and M. Rubinstein, *Phys. Rev. Lett.*, 2000, **84**, 3101–3104.
26 D. Volodkin, V. Ball, P. Schaaf, J.-C. Voegel and H. Mohwald, *Biochim. Biophys. Acta, Biomembr.*, 2007, **1768**, 280–290.
27 F. Bordi, C. Cametti, C. Marianecci and S. Sennato, *J. Phys.: Condens. Matter*, 2005, **17**, S3423–S3432.
28 C. Cametti, *Chem. Phys. Lipids*, 2008, **155**, 63–73.
29 F. Bordi, S. Sennato and D. Truzzolillo, *J. Phys.: Condens. Matter*, 2009, **21**, 203102–203128.
30 A. Y. Grosberg, T. T. Nguyen and B. I. Shklovskii, *Rev. Mod. Phys.*, 2002, **74**, 329–345.
31 J. I. Fleer, M. A. Cohen Stuart, J. M. H. M. Scheutjens, T. Cosgrove and B. Vincent, *Polymers at interface*, Chapman and Hall, London,

1993; T. Nylander, Y. Samoshina and B. Lindman, *Adv. Colloid Interface Sci.*, 2006, **123–126**, 105–123.
32 J. Brugnerotto, J. Desbrieres, G. Roberts and M. Rinaudo, *Polymer*, 2001, **42**, 9921–9927; K. Mazeau, S. Perez and M. Rinaudo, *J. Carbohydr. Chem.*, 2000, **19**, 1269–1284.
33 W. F. Reed, *Light scattering results on polyelectrolyte conformation. Diffusion and interparticule interactions and correlations, In Macro-ion characterization from dilute solutions to complex fluids*, ACS symposium series 548, ed. K. Smitz , 1994, pp 297–314; K. Haxaire, I. Braccini, M. Milas, M. Rinaudo and S. Perez, *Glycobiology*, 2000, **10**, 587–594; M. Milas and M. Rinaudo, *Characterization and properties of hyaluronic acid (hyaluronan) in Polysaccharides: structural diversity and functional versatility*, ed. S. Dimitriu, Dekker, New-York, 2005, pp 535–549.
34 M. I. Angelova, S. Soleau, P. Meleard, J.-F. Faucon and P. Bothorel, *Prog. Colloid Polym. Sci.*, 1992, **89**, 127–133.
35 M. J. Hope, M. B. Bally, G. Webb and P. R. Cullis, *Biochim. Biophys. Acta, Biomembr.*, 1985, **812**, 55–65; R. Nayar, M. J. Hope and P. R. Cullis, *Biochim. Biophys. Acta, Biomembr.*, 1989, **986**, 200–206.
36 R. J. Hunter, *Zeta potential in colloid science, principles and applications*, Academic Press, London, 1981.
37 H. I. Petrache, S. Tristram-Nagle, K. Gawrisch, D. Harries, V. A. Parsegian and J. F. Nagle, *Biophys. J.*, 2004, **86**, 1574–1586.
38 G. Hozwarth, *Carbohydr. Res.*, 1978, **66**, 173–186.
39 M. Q. Zhang, T. Desai and M. Ferrari, *Biomaterials*, 1998, **19**, 953–960.
40 T. Portet, F. C. Febrer, J.-M. Escoffre, C. Favard, M.-P. Rols and D. S. Dean, *Biophys. J.*, 2009, **96**, 4109–4121.
41 J. Sabin, G. Prieto, J. M. Ruso, R. Hidalgo-Alvarez and F. Sarmiento, *Eur. Phys. J. E*, 2006, **20**, 401–408.
42 K. Carvalho, L. Ramos, C. Roy and C. Picart, *Biophys. J.*, 2008, **95**(9), 4348–4360; C. C. Campillo, A. P. Schroder, C. M. Marques and B. Pépin-Donat, *Mater. Sci. Eng., C*, 2009, **29**(2), 393–397.
43 R. P. Haugland, *The Handbook. A Guide to Fluorescent Probes and Labeling Technologies*, Invitrogen, San Diego, 10th edn, 2005.
44 E. Fouissac, Ph.D. Thesis, Université Joseph Fourier, Grenoble, France, 1992.
45 M. Rinaudo, G. Pavlov and J. Desbrieres, *Int. J. Polym. Anal. Charact.*, 1999, **5**, 267–276; L. Rusu-Balaita, J. Desbrières and M. Rinaudo, *Polym. Bull.*, 2003, **50**, 91–98.
46 R. Dimova, N. Bezlyepkina, M. Domange Jordö, R. L. Knorr, K. A. Riske, M. Staykova, P. M. Vlahovska, T. Yamamoto, P. Yang and R. Lipowsky, *Soft Matter*, 2009, **5**, 3201–3212.
47 F. Dubreuil, F. Quemeneur, A. Fery, M. Rinaudo and B. Pépin-Donat, unpublished work.
48 S. Kremer, C. Campillo, F. Quemeneur, M. Rinaudo, B. Pépin-Donat and F. Brochard-Wyart, unpublished work.
49 A. Pavinatto, F. J. Pavinatto, A. Barros-Timmons and O. N. OliveiraJr, *ACS Appl. Mater. Interfaces*, 2010, **2**, 246–251.
50 R. Varoqui, *New J. Chem.*, 1982, **6**, 187–189.